

Energy losses due to vortex shedding from the lower edge of a vertical plate attacked by surface waves

BY M. STIASSNIE, E. NAHEER AND IRINA BOGUSLAVSKY
*Coastal and Marine Engineering Research Institute, Technion,
 Haifa 32000, Israel*

(Communicated by F. Ursell, F.R.S. - Received 9 April 1984)

The ratio between the flux of the energy taken out by the vortex generation process e_v , and the incoming wave energy flux e_w , is shown to be given by

$$e_v/e_w \approx 2\alpha^2 / \{\mu[K_1^2(\mu) + \pi^2 I_1^2(\mu)]\}^{\frac{1}{2}},$$

where $\alpha = \nu r_0$ and $\mu = \nu T$ are non-dimensional parameters and K_1, I_1 are modified Bessel functions. The parameters r_0 and ν are the amplitude and wavenumber of the incoming wave, respectively, and T is the draught of the plate. This theoretically derived formula is in good agreement with experimental evidence.

1. INTRODUCTION

The problem of surface waves diffracting from a vertical plate (see figure 1) was solved analytically by Haskind (1959). For the sake of simplicity we confine the discussion herein to a rigidly held plate and to infinitely deep water. The first published solution for the rigidly held plate was given by Ursell (1947), with the main results expressed in terms of the transmission and reflection coefficients.

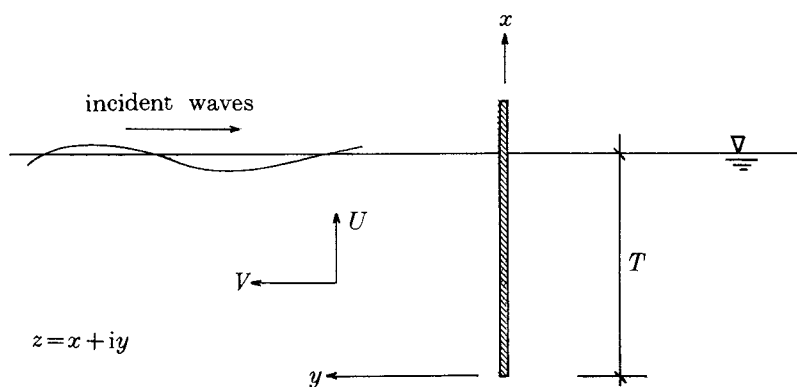


FIGURE 1. Definition sketch for waves approaching a vertical plate.

The transmission coefficient C_t (defined as the transmitted wave to incident wave amplitude ratio), and the reflection coefficient C_r (defined as the reflected wave to incident wave amplitude ratio), are given by

$$C_t = \frac{K_1(\mu)}{[\pi^2 I_1^2(\mu) + K_1^2(\mu)]^{\frac{1}{2}}}, \quad C_r = \frac{\pi I_1(\mu)}{[\pi^2 I_1^2(\mu) + K_1^2(\mu)]^{\frac{1}{2}}} \quad (1.1 a, b)$$

K_1 and I_1 are modified Bessel functions; $\mu = \nu T$, where ν is the wavenumber and T the draught of the plate. The theoretical results together with our experimental data are plotted in figure 2. One significant difference between the non-dissipative theoretical model and the experiments is the fact that

$$1 - (C_r^2 + C_t^2) = \begin{cases} 0, & \text{theoretical result} \\ e_1/e_w, & \text{experimental result} \end{cases}, \quad (1.2)$$

where e_1 is the total power loss between the upstream and the downstream measuring stations, and e_w is the incident wave energy flux (power). The relative energy loss e_1/e_w is shown at the bottom of figure 2 and it appears to vary between 5% and 18%.

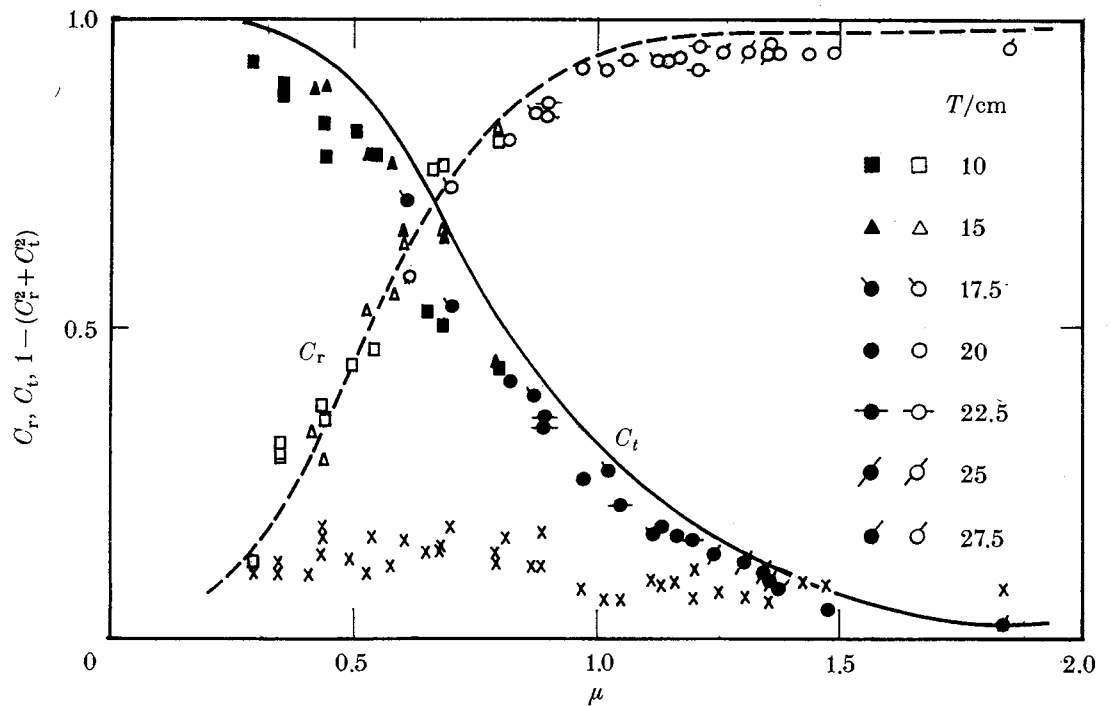


FIGURE 2. Reflection and transmission coefficients for a rigidly held vertical plate. Full symbols are for transmission; hollow symbols are for reflection; the crosses are for energy dissipation.

It is a well known fact that sharp edges, like the one at the origin (0, 0), cause boundary layer separation and tend to shed vortices (see figure 7 in Knott & Mackley (1980)). These vortices are shed in pairs, one pair per wave period, and move downward and away from the edge. The assumption that only one pair of vortices is shed during one wave period is verified in the Appendix. The kinetic energy of the vortices, which is eventually converted into heat by viscous dissipation, is one reason for $e_1 \neq 0$. For experiments made in relatively narrow wave flumes

$$e_1 = e_v + e_f, \quad (1.3)$$

where e_v is a result of the vortex formation and e_f is a result of the viscous friction

near the side walls. The objective of the present paper is to provide a quantitative assessment to the amount of energy that is transferred from the waves to the vortices.

2. THEORY

Vortex coordinates and circulation

To simplify the analysis we confine our interest to a single vortex only, thus neglecting the influence of the previously shed vortices.

Following Haskind (1959), one can show that the wave field velocity near the origin is given by

$$W_w = U_w - iV_w = \gamma(t)/z^{\frac{1}{2}} + O(z^0), \quad (2.1)$$

$$\text{where } \gamma(t) = \frac{\sigma r_0 [K_1(\mu) \cos(\sigma t + \epsilon) + \pi I_1(\mu) \sin(\sigma t + \epsilon)]}{[K_1^2(\mu) + \pi^2 I_1^2(\mu)] (2\mu\nu)^{\frac{1}{2}}}. \quad (2.2)$$

Here, t is the time, r_0 is the incoming wave amplitude, ϵ is the phase shift and $\sigma = (g\nu)^{\frac{1}{2}}$ is the frequency. The square-root singularity at the edge of the plate is unacceptable on physical grounds and one should try to eliminate it. Using a method similar to the one used to solve the lifting problem in ¶5.7 of Newman (1977), one can show that the complex velocity field of a vortex (with centre at x_v, y_v) in the presence of a semi-infinite plate (located on the positive real axis) is given by

$$W_v = \frac{i\Gamma}{2\pi} \frac{1}{z_v - z} + \frac{i\Gamma}{2\pi(z_v^{\frac{1}{2}} - (z_v^{\frac{1}{2}})^*)} \left[1 - \frac{z - x_v}{(z^{\frac{1}{2}} - z_v^{\frac{1}{2}})(z^{\frac{1}{2}} - (z_v^{\frac{1}{2}})^*)} \right] \frac{1}{z^{\frac{1}{2}}}, \quad (2.3)$$

where i is the imaginary unit and the asterisk denotes the complex conjugate. Note that W_v , too, has a square-root singularity at the origin $z = 0$. To eliminate the singularity we apply the so-called Kutta condition, namely $\lim_{z \rightarrow 0} (W_w + W_v) = O(1)$, which yields

$$\gamma(t) + \frac{i\Gamma(1 + x_v/|z_v|)}{2\pi(z_v^{\frac{1}{2}} - (z_v^{\frac{1}{2}})^*)} = 0. \quad (2.4)$$

It is well known that the location of the centre of a mature vortex (i.e. one with fixed circulation) is governed by the equation

$$dz_v^*/dt = \lim_{z \rightarrow z_v} [W - i\Gamma/2\pi(z_v - z)],$$

where W (in our case $W = W_w + W_v$) is the overall complex velocity.

For a vortex in process of generation, a *condition* equivalent to the above zero force condition is required to complete the specification of the vortex and its path.

Since this point vortex represents a growing spiral vortex sheet attached to the edge of the plate, the point z_v must be joined to the origin by a cut representing the sheet. This point vortex plus cut is the simplified model first suggested by Brown & Michael (1955) to represent the spiral vortex above the leading edge of

a slender wing. A suitable *condition* can be derived by considering the condition of zero total force on the vortex plus the cut,

$$\frac{d}{dt}(\Gamma z_v^*) = \lim_{z \rightarrow z_v} \left\{ \Gamma \left[W - \frac{i\Gamma}{2\pi(z_v - z)} \right] \right\} = \frac{\Gamma^2 y_v}{4\pi z_v (z_v^{\frac{1}{2}} - (z_v^{\frac{1}{2}})^*)^2} - \frac{i\Gamma^2 x_v}{2\pi |z_v| z_v^{\frac{1}{2}} (z_v^{\frac{1}{2}} - (z_v^{\frac{1}{2}})^*)}. \quad (2.5)$$

Equation (2.5) is the time dependent analogue of the equation used by Brown & Michael (see, also, Graham 1977).

Equation (2.4), which is real, together with (2.5), which is complex, constitute a set of three real equations for the three real unknowns, Γ , x_v and y_v . The solution of this set for the initial conditions $x_v = y_v = \Gamma = 0$ at $t = 0$, is

$$\Gamma = -2\sqrt{2\pi\gamma} \left(\frac{1}{2\sqrt{2\gamma}} \int_0^t \gamma^2 dt \right)^{\frac{1}{3}}, \quad (2.6a)$$

$$y_v = \left(\frac{1}{2\sqrt{2\gamma}} \int_0^t \gamma^2 dt \right)^{\frac{2}{3}}, \quad (2.6b)$$

$$x_v = 0, \quad (2.6c)$$

If one chooses ϵ in (2.2) so that $V_w > 0$ for t in $(0, \pi\sigma^{-1})$, then γ can be rewritten as

$$\gamma(t) = \sigma C \sin \sigma t, \quad \text{where } C = r_0 / [2\mu\nu(K_1^2 + \pi^2 I_1^2)]^{\frac{1}{2}}. \quad (2.7)$$

With this notation (2.6a) and (2.6b) become

$$\Gamma = -2\pi\sigma C^{\frac{1}{3}} \sin^{\frac{2}{3}}(\sigma t) \left[\frac{1}{2}\sigma t - \frac{1}{4}\sin(2\sigma t) \right]^{\frac{1}{3}}, \quad (2.8a)$$

$$y_v = \left\{ \frac{C}{2\sqrt{2}\sin(\sigma t)} \left[\frac{\sigma t}{2} - \frac{\sin(2\sigma t)}{4} \right] \right\}^{\frac{2}{3}}. \quad (2.8b)$$

The function $\Gamma(t)$ has one maximum, denoted by Γ_m , in the interval $(0, \pi\sigma^{-1})$ and we assume it is not much different from the circulation at the mature state.

One can show that this maximum occurs at $t = t_m$, where $\sigma t_m = 1.94$ and that Γ_m and $y_m = y_v(t_m)$ are given by

$$\Gamma_m / r_0^2 = -3.95 [(\nu r_0) \mu (K_1^2 + \pi^2 I_1^2)]^{-\frac{2}{3}}, \quad (2.9a)$$

$$y_m / r_0 = 0.45 [(\nu r_0) \mu (K_1^2 + \pi^2 I_1^2)]^{-\frac{1}{3}}. \quad (2.9b)$$

Energy estimate

It is only fair to warn the reader that the estimation of the vortex energy seems to be the most difficult, as well as shaky, part of the theoretical approach. In the present section we rely more often on intuition (whatever this stands for!) than on sound theory. To be more specific, the imposed assumptions are

- (i) the irrotational vortex is replaced by a viscous core vortex;
- (ii) while calculating the energy of the vortex, its interactions with the wave field, as well as with the plate, are ignored;
- (iii) the range of integration is limited to $|z - z_v| < y_m$.

The circumferential velocity of a viscous core line vortex is

$$v = \Gamma_m (1 - e^{-r^2/4\tilde{\nu}\tau}) / 2\pi r, \quad (2.10)$$

where $r = |z - z_v|$, $\tilde{\nu}$ is the kinematic viscosity and τ is time (see Rott 1958).

To assign a plausible value for τ we require that the circumferential velocity at $r = y_m$ (i.e. at a distance equal to that between the vortex centre and the edge of the plate, at t_m) as given by the above viscous core vortex, should be identical to the circumferential velocity of an irrotational vortex given by $v = \Gamma_m/2\pi r$. Since these velocities cannot be made identical we have chosen to tolerate a relative difference of 1%, which leads to $\exp(-y_m^2/4\tilde{\nu}\tau) = 0.01$ and thus to $\tau = y_m^2/16.4\tilde{\nu}$. It turns out, as we show later, that choosing a relative difference of 0.001, instead of 0.01, has only a minor effect on the final result.

The energy flux from the wave field into the vortex motion is approximated by

$$e_v = \frac{\sigma}{\pi} \rho 2\pi \int_0^{y_m} v^2 r dr = 0.54 \frac{\rho \sigma^3 r_0^4}{[(\nu r_0) \mu (K_1^2 + \pi^2 I_1^2)]^{3/4}}. \quad (2.11)$$

The incoming wave energy flux is

$$e_w = \frac{1}{4\sigma} \rho g^2 r_0^2. \quad (2.12)$$

From (2.11) and (2.12) we obtain

$$\frac{e_v}{e_w} = D \frac{(\nu r_0)^{3/4}}{[\mu (K_1^2 + \pi^2 I_1^2)]^{3/4}}. \quad (2.13)$$

The numerical value obtained for D is 2.16. If we assume $\exp(-y_m^2/4\tilde{\nu}\tau) = 0.001$, instead of 0.01, D would be 2.79 instead of 2.16.

3. EXPERIMENTAL VERIFICATION

The model

Tests were made in a 27 m long, 60 cm wide and 1.30 m deep wave channel. The channel is equipped with a piston-type wave generator, the motion of which is controlled by an external (electronic) signal. For the present investigation, sinusoidal signals were used to generate monochromatic waves. An absorbing beach made of rubberized hair and having a slope of 1:3 was installed at the downstream end of the channel.

The 1 cm thick plywood plate, which spanned from wall to wall across the channel, was rigidly fixed at a distance of 14 m from the wave generator to the channel concrete walls. The gaps between the plate and the walls were sealed. Tests were made at various plate draughts from 10 to 25 cm at water depths from 62.5 to 77.5 cm.

Waves were measured with resistance-type gauges. The data were accumulated by a computer and directly analysed by using a method similar to that of Knott & Flower (1979). In this method, a pair of wave gauges on each side of the plate is sufficient to estimate the amplitudes of incident, reflected, transmitted and beach-reflected waves. To reduce uncertainties due to measurement errors, four gauges were used on each side and the results that were obtained from various combinations of wave gauge pairs were averaged. The gauges in the group were placed at unequal spacings in an approximately 1 m long section along the channel. Since measurement errors may be augmented when the distance between two wave

gauges is close to an integer multiple of half the wavelength, the wave gauge pairs having near-critical distances were discarded from the computations, thus reducing the possibility of substantial measurement errors.

The distances from the centres of the wave gauge groups to the plate were approximately 2 m. Various wavelengths were employed with maximum values limited by approximately twice the water depth, to keep the waves in the deep water régime.

Results

Preliminary analysis of raw data

As a first approximation it was assumed that $e_f \ll e_v$ (see equation (1.3)), i.e., $e_1/e_w \approx e_v/e_w$. Then from (1.2) and (2.13) one obtains

$$1 - (C_r^2 + C_t^2) = \frac{D\alpha^3}{\{\mu[K_1^2(\mu) + \pi^2 I_1^2(\mu)]\}^{3/2}}, \quad (3.1)$$

where $\alpha = vr_0$. Equation (3.1) describes a family of curves for various values of α in the $(e_v/e_w) - \mu$ plane. The graphical presentation is reduced to a single curve by showing $(e_v/e_w)/\alpha^3$ as a function of μ . The results are shown in figure 3, where the theoretical curve was calculated assuming a value of 2.16 for D .

From figure 3 it seems that the theory has the same trend as the experimental results, but otherwise the data points are widely scattered and the agreement is rather poor. The trend of results indicates the correctness, in principle, of the

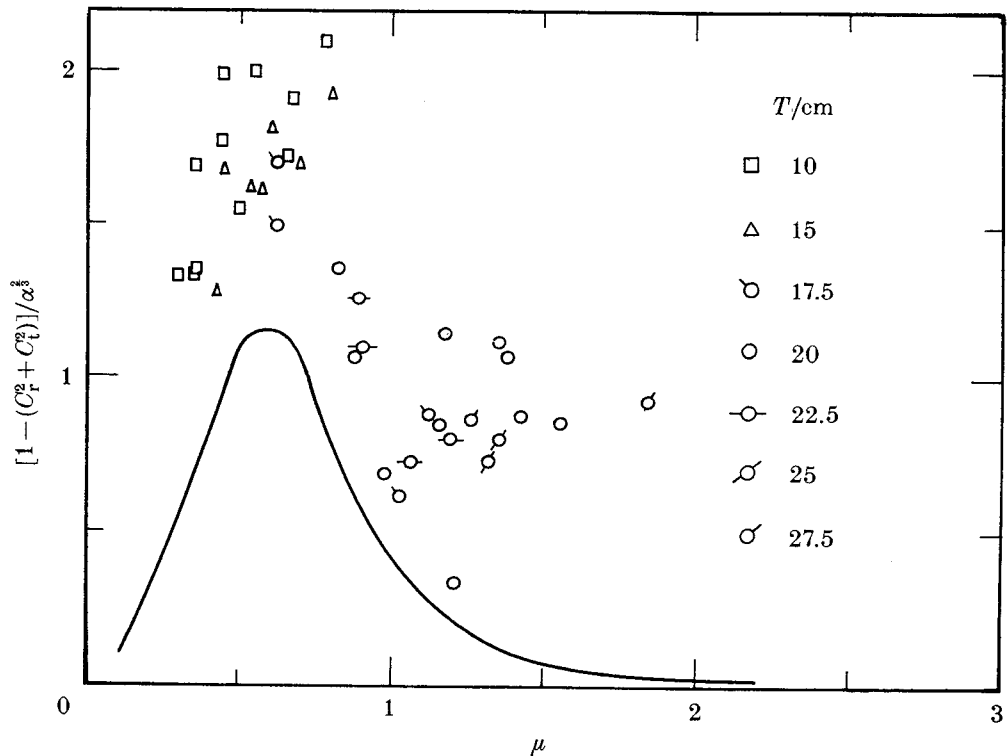


FIGURE 3. Energy dissipation for a rigidly held plate.

theoretical considerations. The large data scatter and the fact that these data are higher than the theoretical values may be explained by the following points.

(i) The higher experimental values are possibly due to a value for D that is too low. A higher value would bring the theoretical curve closer to the experimental results, but at $\mu > 1.0$ the experimental values would still be much higher than the theory.

(ii) The experimental scatter is possibly due to measurement errors. A reasonable error in the measurement of C_r and C_t becomes increasingly large compared to the very small quantity $1 - (C_r^2 + C_t^2)$.

(iii) Energy losses other than by vortex formation are possibly responsible for both the higher experimental results and the apparently large scatter of data. These losses (i.e. e_f) were neglected in the above analysis. Including them in the analysis yields

$$1 - (C_r^2 + C_t^2) - \frac{e_f}{e_w} = \frac{D\alpha^{\frac{3}{2}}}{\{\mu[K_1^2(\mu) + \pi^2 I_1^2(\mu)]\}^{\frac{4}{3}}}; \quad (3.2)$$

cf. (1.2), (4.3) and (2.13).

The effects of frictional losses were employed as described later.

Application of wave attenuation

Consider the experimental arrangement shown schematically in figure 4. The distance between the two measurement stations is d and the plate is placed at exactly the midpoint between them. Waves at the measurement stations and near the plate are denoted by subscripts 0 and 1, respectively.

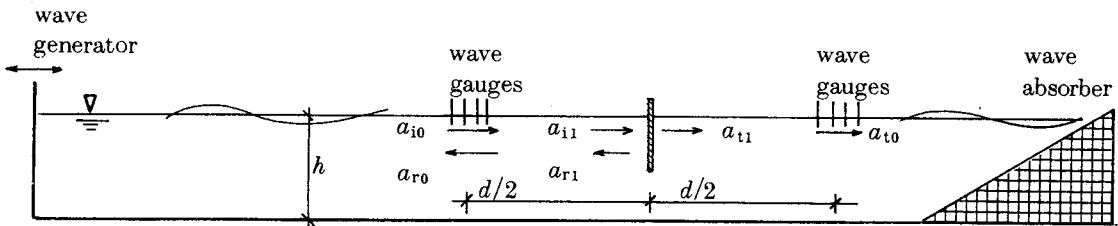


FIGURE 4. Definition sketch for correction of results due to attenuation of waves.

The amplitudes a_{i1} , a_{r1} and a_{t1} cannot be measured experimentally since the wave motion in the vicinity of the plate is complicated by local phenomena.

They are assumed to be given by

$$a_{i1} = a_{i0} \epsilon_{d/2}(a_i), \quad (3.3a)$$

$$a_{t1} = a_{t0} / \epsilon_{d/2}(a_t), \quad (3.3b)$$

$$a_{r1} = a_{r0} / \epsilon_{d/2}(a_r), \quad (3.3c)$$

where $\epsilon_{d/2}(a)$ is the attenuation coefficient for a wave of amplitude a travelling a distance $\frac{1}{2}d$.

The measured coefficients of transmission and reflection are defined by

$$C_t = a_{t0} / a_{i0}, \quad (3.4a)$$

$$C_r = a_{r0} / a_{i0}, \quad (3.4b)$$

and the corrected coefficients by

$$C_t^* = a_{t1}/a_{i1}, \quad (3.5a)$$

$$C_r^* = a_{r1}/a_{i1}. \quad (3.5b)$$

Substitution of (3.3) in (3.4) and with use of (3.5) yields

$$C_t = \epsilon_{d/2}(a_i) \epsilon_{d/2}(a_t) C_t^*, \quad (3.6a)$$

$$C_r = \epsilon_{d/2}(a_i) \epsilon_{d/2}(a_r) C_r^*. \quad (3.6b)$$

The attenuation of wave amplitude along the channel was measured for the two following cases: (i) waves propagating freely in an obstacle-free channel; (ii) waves reflected from a vertical rigid wall that blocks the channel completely.

For the first case, the wave is measured at two stations (consisting of four wave gauges each) located at a distance of 4.2 m from each other. In the second, the distance from the measurement station to the wall was 2.1 m so that the distance the wave travelled from the station to the wall and back was also 4.2 m.

The results showing the coefficient of energy attenuation ϵ_d^2 , as a function of the wave number, ν , for waves of various amplitudes travelling a distance $d = 4.2$ m are presented in figure 5. Also shown in this figure is the theoretical curve for infinitesimal waves ($a = 0$), as developed by Hunt (1952).

If we assume that the attenuation of wave amplitude along a distance x is given by

$$a_x = a_0 e^{-\beta x}, \quad (3.7)$$

where β is a (constant) damping coefficient, then the relation between the attenuation coefficients for waves travelling distances d and $\frac{1}{2}d$ is

$$\epsilon_{d/2} = \epsilon_d^{\frac{1}{2}}. \quad (3.8)$$

From (3.8) and (3.6) the final result

$$C_t^* = C_t / [\epsilon_d(a_i) \epsilon_d(a_t)]^{\frac{1}{2}}, \quad (3.9a)$$

$$C_r^* = C_r / [\epsilon_d(a_i) \epsilon_d(a_r)]^{\frac{1}{2}} \quad (3.9b)$$

is obtained. The corrected coefficients, C_t^* , and C_r^* can now be estimated directly, since the right-hand side (3.9) consists of known quantities, which were measured experimentally. The results are shown in figure 6. Compared to figure 2, it can be seen that the experimental results are now a little closer to the theoretical curves. It is interesting that the corrected experimental results display systematic deviation from the theoretical results only for the transmission coefficient, while for reflection the experimental data agree well with the theory. This indicates that energy dissipation is involved only in the transmission mechanism, and not in the reflection (such an observation was also made by Knott & Mackley (1980)).

After correcting the results for energy dissipation, the energy balance can now be written in the form

$$e_v/e_w = 1 - (C_r^{*2} + C_t^{*2}) \quad (3.10)$$

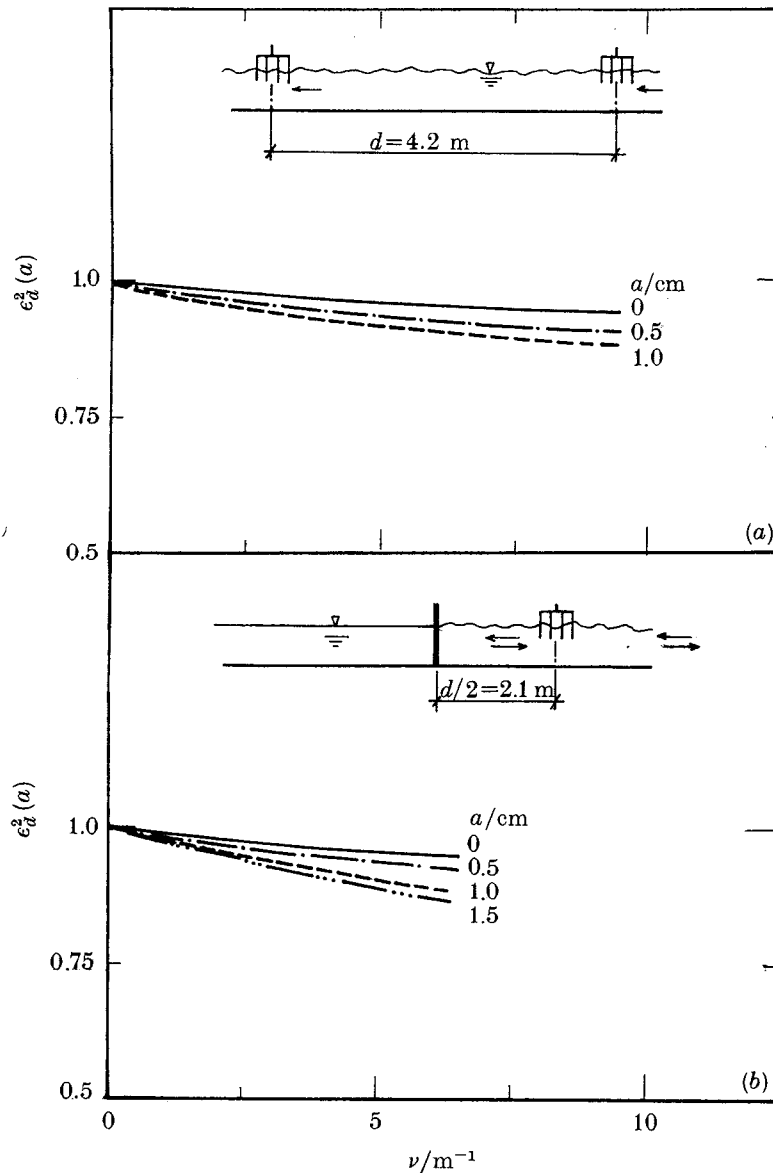


FIGURE 5. Viscous dissipation of waves in a 60 cm wide channel. $h = 0.725$ m; $d = 4.2$ m; (a) obstacle-free channel; (b) totally reflected waves.

and, by substituting (3.9),

$$\frac{e_v}{e_w} = 1 - \frac{1}{\epsilon_d(a)} \left[\frac{C_t^2}{\epsilon_d(a_t)} + \frac{C_r^2}{\epsilon_d(a_r)} \right]. \quad (3.11)$$

The theoretical value (equation (2.13)) is now compared in figure 7 to the corrected value (equation (3.11)), which represents the experimental measurements.

The scatter of data in figure 7 is most certainly due to measurement errors, but the improvement over the original, uncorrected results (figure 3) is impressive. The agreement between the theory and experiments supports the theoretical approach.

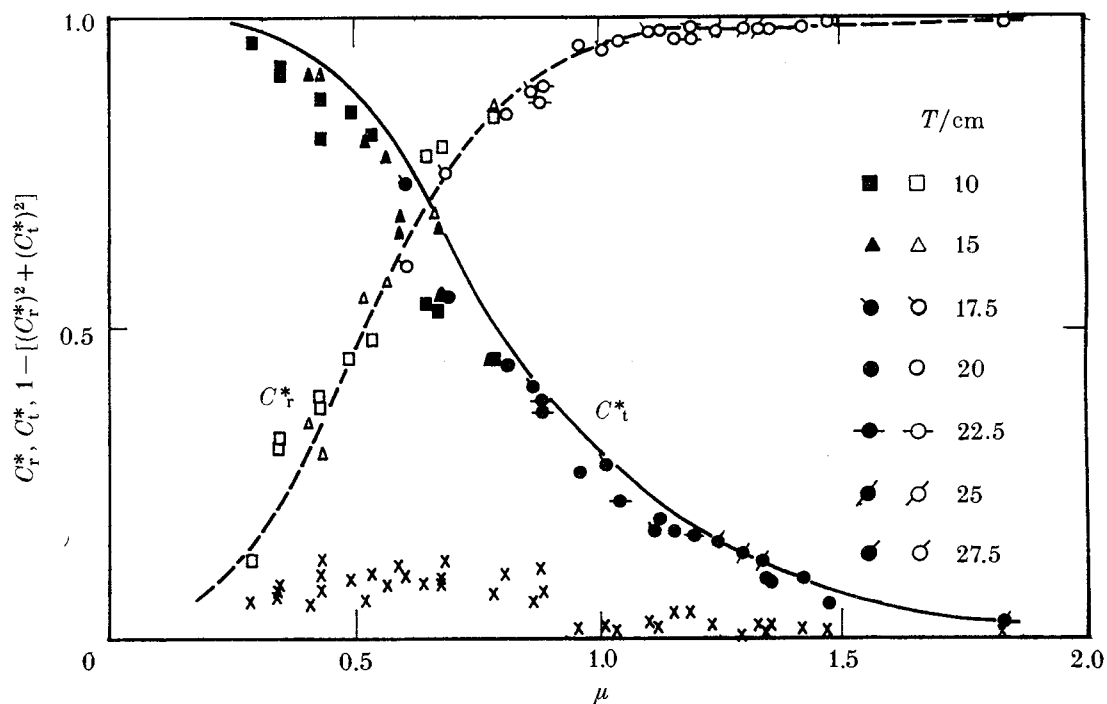


FIGURE 6. Reflection and transmission coefficients for a rigidly held plate, corrected for viscous dissipation. Full symbols are for transmission; hollow symbols are for reflection; the crosses are for energy dissipation.

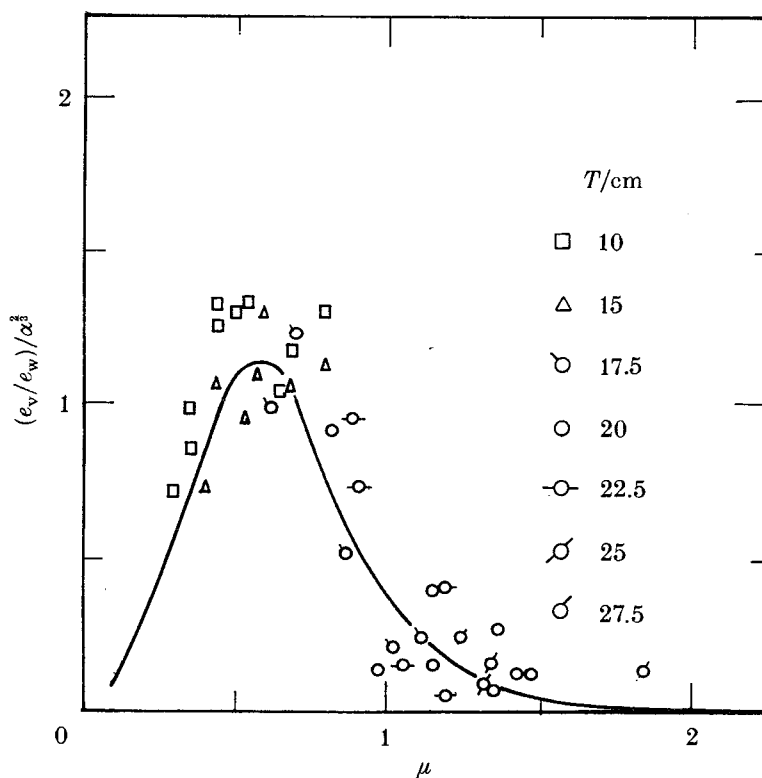


FIGURE 7. Energy dissipation for a rigidly held plate, corrected for viscous dissipation.

APPENDIX

Throughout the analysis, we have assumed that only one pair of vortices is shed per wave period. In the following, we bring some reasonings to show that it is indeed so for any possible α provided $\mu > 0.2$. When $\mu < 0.2$, α is limited by the condition $\alpha < 2\mu$.

Fage & Johansen (1927) have shown that the frequency with which the individual vortices leave each edge of a flat plate of breadth $2a$ in a perpendicular stream of undisturbed velocity U is given by

$$f = 0.146U/2a. \quad (\text{A } 1)$$

To apply this result to our problem and to replace U and a by their appropriate equivalents, we introduce two assumptions:

(i) the undisturbed velocities at the edges have to be the same for both problems:

$$U = \sigma r_0 e^{-\mu}; \quad (\text{A } 2)$$

(ii) the singularities at the edges ought to have the same strength,

$$U(a/2)^{\frac{1}{2}} = \sigma C = \sigma r_0/[2\mu\nu(K_1^2 + \pi^2 I_1^2)]^{\frac{1}{2}}. \quad (\text{A } 3)$$

By eliminating U and a from (A 2) and (A 3), and by substituting them into (A 1),

$$f = [0.073\alpha\mu(K_1^2 + \pi^2 I_1^2) e^{-3\mu}] \sigma. \quad (\text{A } 4)$$

To obtain only one pair of vortices per wave period, we need

$$f < \sigma/2\pi, \quad (\text{A } 5)$$

which together with (A 4) gives

$$0.5\alpha\mu e^{-3\mu}(K_1^2 + \pi^2 I_1^2) < 1. \quad (\text{A } 6)$$

Since the wave steepness α is limited by the condition $\alpha < 0.4$, one can show that the inequality (A 6) is satisfied as long as $\mu > 0.2$. For smaller μ , using series expansion of the Bessel function, we obtain

$$0.5\alpha/\mu < 1. \quad (\text{A } 7)$$

REFERENCES

- Brown, C. E. & Michael, W. H. 1955 On slender delta wings with leading-edge separation. *Tech. Notes natn advis. Comm. Aeronaut.* **3430**.
- Fage, A. & Johansen, F. C. 1927 On the flow of air behind an inclined flat plate of infinite span. *Proc. R. Soc. Lond. A* **116**, 170.
- Graham, J. M. R. 1977 Vortex shedding from sharp edges. *Imperial College Aero. Rep.* no. 77-06 (22 pages).
- Haskind, M. D. (Khaskind) 1959 Radiation and diffraction of surface waves from a vertically floating plate. *Prikl. Mat. Mekh.* **23**, 546.
- Hunt, J. N. 1952 Viscous damping of waves over an inclined bed in a channel of finite width. *La Houille Blanche* **7**, 836.
- Knott, G. F. & Flower, J. O. 1979 Wave-tank experiments on an immersed parallel-plate duct. *J. Fluid Mech.* **90**, 327.

- Knott, G. F. & Mackley, M. R. 1980 On eddy motions near plates and ducts, induced by water waves and periodic flows. *Phil. Trans. R. Soc. Lond. A* **294**, 599.
- Newman, J. N. 1977 *Marine hydrodynamics* (402 pages). M.I.T. Press.
- Rott, N. 1958 On the viscous core of a line vortex. *Z. Angew. Math. Phys.* **9b**, 543.
- Ursell, F. 1947 The effect of a fixed vertical barrier on surface waves in deep water. *Proc. Camb. phil. Soc.* **43**, 374.